

MODELLING THREE-PHASE FLOW IN METALLURGICAL PROCESSES

Christoph GONIVA^{1,2*}, Gijsbert WIERINK⁴, Kari HEISKANEN⁴, Stefan PIRKER^{2,3} and Christoph KLOSS^{1,2}

¹DCS Computing GmbH, Linz, AUSTRIA

²Christian-Doppler Laboratory on Particulate Flow Modelling, Johannes Kepler University, Linz, AUSTRIA

³Institute of Fluid Mechanics and Heat Transfer, Johannes Kepler University, Linz, AUSTRIA

⁴Mechanical Process Technology and Recycling, Aalto University, Espoo, FINLAND

*Corresponding author, E-mail address: christoph.goniva@jku.at

ABSTRACT

The interaction between gasses, liquids, and solids plays a critical role in many processes, such as coating, granulation and the blast furnace process. In this paper we present a comprehensive numerical model for three phase flow including droplets, particles and gas. By means of a coupled Computational Fluid Dynamics (CFD) - Discrete Element Method (DEM) approach the physical core phenomena are pictured at a detailed level. Sub-models for droplet deformation, breakup and coalescence as well as droplet-particle and wet particle-particle interaction are applied. The feasibility of this model approach is demonstrated by its application to a rotating drum coater. The described numerical model is implemented completely in an open source framework developed and provided by the authors.

NOMENCLATURE

Greek symbols

α volume fraction (-)

ν_p Poisson ratio (-)

λ_f bulk viscosity (kg/(m s))

μ_c Coulomb friction coefficient (-)

μ_f gas phase shear viscosity (kg/(m s))

μ friction coefficient (-), dynamic viscosity (kg/(m s))

ρ density (kg/m³)

σ surface tension (N/m)

τ stress tensor (Pa)

ω angular velocity (1/s)

Latin symbols

c damping coefficient (kg/s)

C_d drag coefficient (-)

d diameter (m)

e coefficient of restitution (-)

F force exerted on a single particle (N)

g gravity vector (m/s²)

I identity matrix (-)

K momentum exchange coefficient (kg/(m³ s))

k spring stiffness (N/m)

m mass (kg)

N number (cells, particles) (-)

p pressure (Pa)

r radius (m)

R momentum source term (N/m³)

R_μ rolling friction model parameter (-)

Re Reynolds number (-)

T torque (Nm)

t time (step) (s)

u velocity (m/s)

Δu_p relative particle velocity at contact point (m/s)

V volume (m³)

x position (m)

x, y, z Cartesian-coordinates (-)

Δx particle overlap at contact point (m)

Y Young's modulus (Pa)

Sub/superscripts

c contact

f fluid

n normal to contact point

p particle

t tangential to contact point

rel relative

INTRODUCTION

The interaction between gasses, liquids, and solids plays a critical role in many processes, such as coating, granulation and the blast furnace process to name a few. Control and manipulation of the interaction between phases is of key interest in engineering practise. Typically, industrial applications are of such a scale that detailed modelling is generally not feasible, while governing processes are characterised by length and time scales that are many orders of magnitudes smaller than those of the unit process. In this light the understanding and modelling of governing phenomena on an intermediate temporal and spatial scale can deepen understanding of the unit process at an industrial scale.

During the last years several models for three phase flow mostly applied to granulation or coating can be found. Most of them used a DEM approach in combination with a residence time within a spray region to capture the effect of droplet-particle liquid transfer (Fries et al. 2011; Dubey et al. 2011; Sahni et al. 2011), an assumption which strictly holds only if the spray is not influenced by the fluid flow. The coating and granulation process in fluidized bed reactors modelled by coupled CFD-DEM

method was highlighted by Fries (2011), Darabi (2011) and van Buijtenen (2008). A DEM based droplet-particle interaction approach was presented by Goldschmidt et al (2003). A very detailed model for the liquid transfer between particles as well as capillary and viscous forces of the liquid bridges was given by Shi and McCarthy (2008). More simplified models for the effect of liquid bridges on particle contacts were given by Darabi et al. (2007) and van Buijtenen et al. (2008).

This paper highlights the modelling of droplet-particle interaction at the intermediate scale, the so-called meso-scale, by a coupled Computational Fluid Dynamics (CFD) - Discrete Element Method (DEM) approach. While the liquid phase, which is present as droplets, is treated by a parcel-based approach, the granular phase is resolved by DEM and the interstitial fluid is modelled by CFD, solving the volume averaged Navier-Stokes Equations.

In a first section the governing equations for this model approach are discussed. Effects like droplet deformation, droplet break-up, droplet coalescence are pictured by dedicated sub-models available in literature. Liquid transfer between droplets and the particles is handled efficiently by a Eulerian-Lagrangian approach. Particle-particle liquid transfer as well as the effect of liquid bridges on particle contact physics is treated by sub-routines within the DEM. The feasibility of this model approach is demonstrated by its application to a rotating drum coater. Finally a conclusion and an outlook of this work are given.

MODEL DESCRIPTION

The method presented here resolves the fluid and particle calculations by two strictly separated codes. The interaction is realised by exchange fields being evaluated in a predefined time interval, where the codes work in a sequential manner. Both the CFD and the DEM code do their calculations in parallel using Message Passing Interface (MPI) parallelisation. Also data exchange between the codes is realised using MPI functionality.

This comprehensive model for three phase flow is realised in a modular approach, where distinct physical phenomena are treated by dedicated sub-models. In this section the governing equations of all subroutines of this model approach will be highlighted.

DEM Method

The Discrete Element Method was introduced by Cundall and Strack (1979). A very brief description of the method will be provided in this section. Further details on the contact physics and implementation issues are available in the literature (e.g. Di Renzo & Di Maio, 2004; Poeschel & Schwager, 2005; Zhu et al., 2007).

The strength of the DEM lies in its ability to resolve the granular medium at the particle scale, thus allowing for realistic contact force chains and giving rise to phenomena induced by particle geometry combined with relative particle motion, such as particle segregation by percolation. Thereby, the DEM is able to capture many different physical phenomena, such as dense and dilute particulate regimes, rapid- as well as slow granular flow and equilibrium states or wave propagation within the granular material.

Thanks to advancing computational power, the DEM has become more and more accessible lately. On actual desktop computers, simulations of up to a million particles can be performed. On very large clusters, the trajectories

of hundreds of millions of particles can be computed (e.g. LAMMPS, 2009).

Governing Equations

In the framework of the DEM, all particles in the computational domain are tracked in a Lagrangian way, explicitly solving each particle's trajectory, based on the force and torque balances:

$$\mathbf{m}_p \ddot{\mathbf{x}}_p = \mathbf{F}_{p,n} + \mathbf{F}_{p,t} + \mathbf{F}_{p,f} + \mathbf{F}_{p,p} + \mathbf{F}_{p,v} + \mathbf{F}_{p,b} \quad (1)$$

and

$$\mathbf{I}_p \frac{d\boldsymbol{\omega}_p}{dt} = \mathbf{r}_{p,c} \times \mathbf{F}_{p,t} + \mathbf{T}_{p,r} \quad (2)$$

where $\mathbf{F}_{p,n}$ is the normal contact force, $\mathbf{F}_{p,t}$ is the tangential contact force. $\mathbf{F}_{p,f}$ is the drag force exerted from the fluid phase to the particles, $\mathbf{F}_{p,p}$ and $\mathbf{F}_{p,v}$ denote respectively the pressure and viscous force acting on the particles. Other body forces like gravity, electrostatic or magnetic forces are lumped into $\mathbf{F}_{p,b}$. For sake of completeness, these forces are described in detail in Table 1.

Forces	Correlations
$\mathbf{F}_{p,n}$	$-k_n \Delta \mathbf{x}_p + c_n \Delta \mathbf{u}_{p,n}$
$\mathbf{F}_{p,t}$	$\min \left\{ \left k_t \int_{t_{c0}}^t \Delta \mathbf{u}_{p,t} dt + c_t \Delta \mathbf{u}_{p,t} \right , \mu_c F_{p,n} \right\}$
$\mathbf{F}_{p,b}$	$\mathbf{g} m_p$
$\mathbf{T}_{p,r}$	$R_\mu k_n \Delta \mathbf{x}_p \frac{\boldsymbol{\omega}_{rel}}{ \boldsymbol{\omega}_{rel} } \frac{d}{2}$
$\boldsymbol{\omega}_{rel}$	$\frac{\mathbf{r}_{p,ci} \boldsymbol{\omega}_{p,i} + \mathbf{r}_{p,cj} \boldsymbol{\omega}_{p,j}}{\mathbf{r}_{p,ci} + \mathbf{r}_{p,cj}}$
$\mathbf{F}_{p,p}$	$-\nabla(p) V_p = (1/2 \rho_f \nabla \mathbf{u}_f^2) V_p + \rho_f \mathbf{g} V_p$
$\mathbf{F}_{p,v}$	$-\nabla \cdot (\boldsymbol{\tau}) V_p$
$\mathbf{F}_{p,f}$	\mathbf{F}_D^*

*Drag force \mathbf{F}_D is explained in Goniva et al. (2012)

Table 1: Components of forces and torques acting on particle p.

Each physical particle is mathematically represented by a sphere, another geometrically well-defined volume or a combination of them. The translational and angular accelerations of a sphere are based on the corresponding momentum balances. Generally, the particles are allowed to overlap slightly. The normal force tending to repulse the particles can then be deduced from this spatial overlap $\Delta \mathbf{x}_p$ and the normal relative velocity at the contact point, $\Delta \mathbf{u}_{p,n}$. The simplest example is a linear spring-dashpot model, shown in Fig. 1.

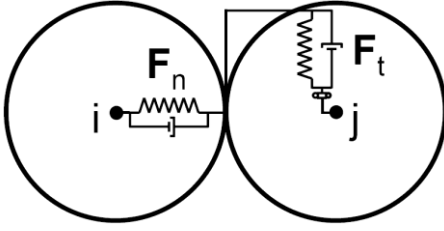


Figure 1 Spring-dashpot model.

An efficient way of taking into account the small-scale non-sphericity of the particles is a rolling friction model, see Goniva et al. (2012). It introduces an additional torque also for collisions, where the relative velocity at the contact point is zero. Within this paper a directional constant torque model (Ai et al., 2011), is applied (see Tab. 1).

CFD-DEM Method

For the modelling of particle laden fluid flow a coupled CFD-DEM approach can be applied (Tsuiji et al. (1993); Deen et al. (2007); Zhu et al. (2008); Zhou et al. (2010)).

Governing Equations

The motion of a fluid phase in the presence of a secondary particulate phase is governed by the volume-averaged Navier-Stokes Equations for compressible fluid, which can be written as:

$$\frac{\partial(\rho_f \alpha_f)}{\partial t} + \nabla \cdot (\rho_f \alpha_f \mathbf{u}_f) = 0, \quad (3)$$

$$\frac{\partial(\rho_f \alpha_f \mathbf{u}_f)}{\partial t} + \nabla \cdot (\rho_f \alpha_f \mathbf{u}_f \mathbf{u}_f) = -\alpha_f \nabla p + \mathbf{R}_{f,p} + \nabla \cdot (\alpha_f \boldsymbol{\tau}_f) + \mathbf{R}_{f,d} \quad (4)$$

Here, α_f is the volume fraction occupied by the fluid, ρ_f is its density, \mathbf{u}_f its velocity, and $\boldsymbol{\tau}_f$ is the stress tensor for the fluid phase. $\mathbf{R}_{f,p}$ represents the momentum exchange with the particulate phase, which is calculated for each cell, where it is assembled from the particle based drag forces. $\mathbf{R}_{f,d}$ represents the momentum exchange with the droplet phase. For solving the above equations a pressure based solver using “Pressure-Implicit Split-Operator” (PISO) pressure-velocity coupling is used, where an implicit momentum predictor followed by a series of pressure solutions and explicit velocity corrections is performed (Jasak, 1996).

CFD-DEM coupling routine

The coupling routine consists of several steps:

- (1) The DEM solver calculates the particle positions and velocities.
- (2) The particle positions, velocities, and other necessary data are passed to the CFD solver.
- (3) For each particle, the corresponding cell in the CFD mesh is determined.
- (4) For each cell, the particle volume fraction as well as a mean particle velocity is determined.
- (5) Based on the particle volume fraction, the fluid forces acting on each particle are calculated.
- (6) Particle-fluid momentum exchange terms are assembled from particle based forces by ensemble averaging over all particles in a CFD cell.

- (7) The fluid forces acting on each particle are sent to the DEM solver and used within the next time step.
- (8) The droplet-particle liquid transfer is calculated.
- (9) The CFD solver calculates the fluid velocity taking into account local particle volume fraction and momentum exchange of the granular and droplet phase.
- (10) Additional equations such as species concentration can optionally be evaluated.
- (11) The routine is repeated from (1).

Fluid-Particle momentum exchange

Once the particle volume fraction is calculated it is possible to evaluate each particle’s contribution to particle-fluid momentum exchange, which is mostly established by means of a drag force depending on the local particle volume fraction.

For numerical reasons the momentum exchange term is split-up into an implicit and an explicit term using the cell-based ensemble averaged particle velocity $\langle \mathbf{u}_p \rangle$:

$$\mathbf{R}_{f,p} = \mathbf{K}_{f,p} \mathbf{u}_f - \mathbf{K}_{f,p} \langle \mathbf{u}_p \rangle, \quad (5)$$

where

$$\mathbf{K}_{f,p} = - \frac{\left| \sum_i \mathbf{F}_{p,f} \right|}{V_{cell} \cdot \left| \mathbf{u}_f - \langle \mathbf{u}_p \rangle \right|}, \quad (6)$$

For the calculation of $\mathbf{K}_{f,p}$ many different drag correlations have been proposed during the recent years (e.g. Zhu et al. (2007)). Within this paper a drag relation based on lattice Boltzmann simulations proposed by Koch and Hill (2001) is used, see Goniva et al. (2012).

Coupled CFD-DEM solver

The coupled CFD-DEM approach described above was implemented within an open source environment (Goniva et al. (2009, 2012); Kloss et al. (2012)). The CFD part of the simulations as well as the Lagrangian droplet tracking is conducted by a solver realised within the open source framework of OpenFOAM® (OpenCFD Ltd., 2009). The coupling routines are collected in a library providing a modular framework for CFD-DEM coupling (CFDEMcoupling, 2011). The DEM part of the simulations is conducted in LIGGGHTS, an open source software package for modelling granular material by means of the Discrete Element Method (LIGGGHTS, 2011). based on LAMMPS, an open source Molecular Dynamics code by Sandia National Laboratories for massively parallel computing on distributed memory machines (Plimpton, 1995).

Both LIGGGHTS and CFDEMcoupling run in parallel using message-passing techniques (MPI) and a spatial-decomposition of the simulation domain. LIGGGHTS and CFDEMcoupling are distributed as open source codes under the terms of the GNU General Public License (GPL). A selection of coupling routines as well as example solvers are provided at a dedicated web page maintained by the authors (CFDEMcoupling, 2011).

Droplet phase

The droplet phase is described in a Lagrangian frame of reference. Since it is impossible to calculate the trajectory of every single droplet within an acceptable time, a

simplification is made. Instead of individual droplets computational ‘parcels’ are traced with each parcel representing a certain mass of droplets that share the same properties (size, velocity, etc.). One could imagine each parcel representing the centre of mass of a cloud of droplets of equal size, following the approach of Crowe et al. (1977).

For the calculation of a parcel’s trajectory a simplified BBO-equation (Basset, Boussinesq, Oseen) is solved:

$$m_D \frac{d\mathbf{u}_D}{dt} = \mathbf{g} m_D + C_{d,D} A_D \frac{\rho_G (\mathbf{u}_G - \mathbf{u}_D) |\mathbf{u}_G - \mathbf{u}_D|}{2}. \quad (7)$$

If the droplet loading is low, which can be assumed in most regions, the volume occupied by the droplets can be neglected. Therefore, the gas phase and the droplets are coupled solely by a source term $\mathbf{R}_{f,d}$ in the gas momentum balance (Eqn. 4) and a drag term in the parcels force balance (Eqn. 7).

Droplet oscillation and break-up

Initial droplets are formed due to primary break-up of a jet or a film. As a result of the shear forces acting on these droplets, they deform and break-up into smaller droplets. A well-known model for droplet break-up is the Taylor Analogy Breakup (TAB) model described by O’Rourke (1987). The model is based on Taylor’s analogy between an oscillating, distorting droplet and a spring-mass-damper system, where the forcing term is given by aerodynamic forces, the damping is due to liquid viscosity and the restoring spring force is supplied by the surface tension. In this model the droplet’s deformation can be determined at any given time by solving a linear differential equation. The deformation of a droplet is described by the deformation parameter $y=(2\Delta r)/r$ as sketched in Fig. 2. As the assumption of spherical droplets is no longer applicable for high Weber numbers, the droplets’ drag coefficient is modelled as a linear interpolation between a sphere and a disc. Besides droplet break-up, collision dynamics is important in the evolution of sprays. Hereby, a model for droplet coalescence and grazing collision, proposed by O’Rourke (see Amsden, 1985), is used. A detailed description of the applied droplet model is given in Goniva et al. (2010).

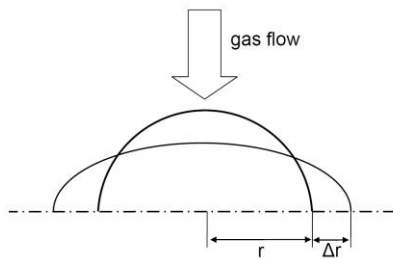


Figure 2 Axisymmetric representation of an oscillating, distorted droplet.

Particle-Particle Liquid Transfer Model

When two particles are in contact, and at least one of them is wet, a liquid bridge will form. Besides capillary and viscous forces resulting from the liquid bridge, a liquid transfer between the particles will occur when the liquid bridge breaks. In a moving granular bed this will lead to a distribution of the liquid. To model the effect of particle-particle liquid transfer we follow the approach proposed by Shi and McCarthy (2008) assuming that: the liquid is evenly distributed on the surface of the particles, resulting from the assumption that the particles are relatively

hydrophilic. The liquid bridge volume is composed of the liquid on the surface of the particles that is within the area of the contact point (Fig. 3). This guarantees conservation of the liquid, as any liquid on the surface of a particle can only contribute to one liquid bridge. From geometrical considerations (Fig. 3) the liquid volume contributed to the liquid bridge from particle I can be written as

$$V_i = \frac{L_i}{2} \times \left(1 - \sqrt{1 - \frac{d_j^2}{(d_i + d_j)^2}} \right), \quad (8)$$

where L_i is the liquid volume, and d_i the diameter of particle i . The liquid bridge volume V_j can be calculated accordingly. The total liquid bridge volume is

$$V = V_i + V_j. \quad (9)$$

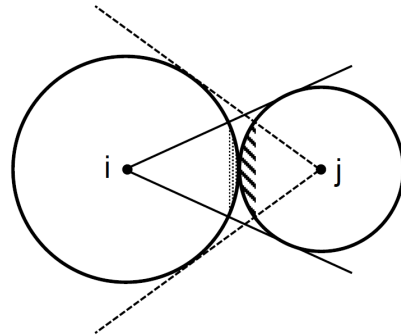


Figure 3: Schematic sketch of spherical cap denoting the liquid contributing to the formation of a liquid bridge.

When the separation distance between the particle surfaces is larger than some critical distance, the liquid bridge will break into droplets remaining with the individual particles. The liquid transfer ratio denoting how the liquid bridge volume is separated depends on the particles diameters and liquid contact angles. Following the approach suggested by Shi and McCarthy (2008) the liquid transfer ratio can be approximated assuming the bridge to have a parabolic shape. For particles of equal size and different liquid contact angles the result is depicted in Fig. 4. For mono-disperse systems with particles of equal liquid contact angle the transfer ratio is 0.5.

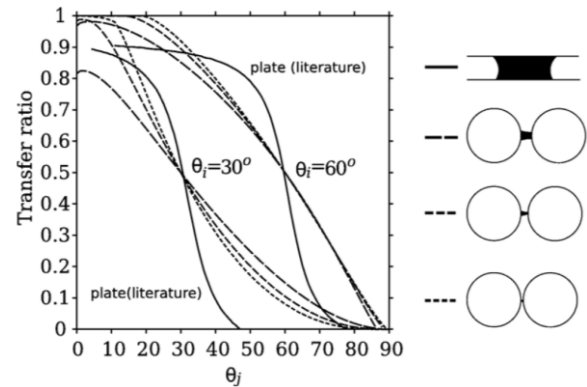


Figure 4: Liquid-bridge transfer ratios depending on the contact angle Θ (left). Differing bridge configurations are shown schematically (at right) with varying line/dash types for two plates; particles with $V=0.001$; particles with $V=0.0001$ and particles with $V=0.00001$., Shi and McCarthy (2008).

The behaviour of the model is shown for two 1mm sized particle bouncing on each other (Fig. 5). Initially particle 1 carries $1e-9$ kg and particle 2 carries 0 kg of liquid on its surface. With each contact some liquid is transferred from particle 1 to particle 2 until a steady state, where both particles carry half the total liquid, is reached.

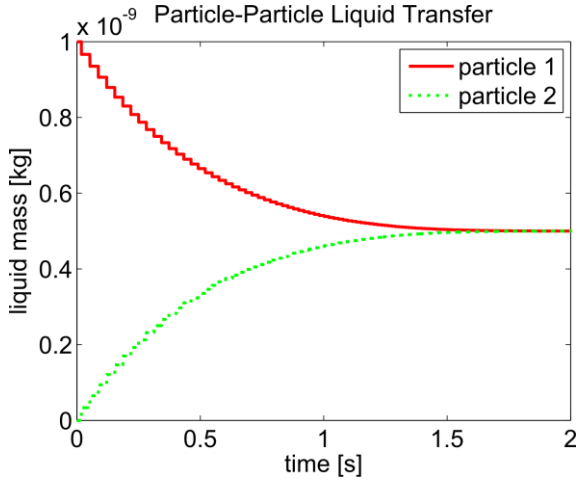


Figure 5: Liquid transfer between a (initially) dry and wet particle bouncing on each other. Both particles have the same liquid contact angle.

Wet Particle-Particle Interaction

The liquid content of two colliding particles affects their interaction, since collisions are less ideal with increasing liquid content. In literature several model approaches different complexities can be found. While Shi and McCarthy (2008) directly calculate the capillary and viscous forces derived from the liquid bridge shape, Darabi et al. (2011) calculate the coefficients of restitution for wet particles modelling the capillary and viscous work. van Buijtenen et al. (2008) suggested a simplified model, blending the dry and wet normal coefficients of restitution depending on the liquid loading.

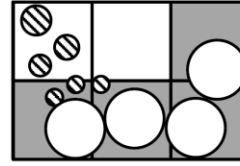
$$e_{n,p} = (e_{n,p0} - e_{n,psat}) \times 10^{-C \frac{m_L}{m_p}}, \quad (10)$$

Where m_L , $e_{n,p0}$, $e_{n,psat}$ denote the liquid mass on the particle surface, the dry normal coefficient of restitution and the normal coefficient of restitution for a saturated particle. The model coefficient C was proposed to be 5.

Droplet-Particle Liquid Transfer

Liquid transfer between droplets and particles is handled efficiently by a combined Eulerian-Lagrangian approach. In a first stage, those droplet parcels which will collide with a particle are detected using the voidfraction field (Fig. 6-a). A Eulerian field marking those areas of droplet-particle liquid transfer is created. Finally, particles located in cells with liquid transfer gain liquid from the Eulerian source field (Fig. 6-b).

a) Liquid Source Detection:



b) Droplet-Particle Transfer:

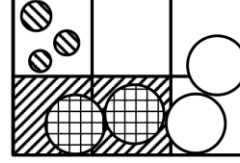


Figure 6: Liquid transfer between droplets and particles, via Eulerian liquid source field.

RESULTS

To illustrate above described modelling approach for three-phase flow including droplets, particles and gas, a very simplified rotating pan coater was simulated. 20000 particles are fed into a rotating drum (length=0.5 m, diameter=0.2m), rotating at 1 Hz. During the first 0.8 seconds 2 ml of water are injected via two vertical nozzles with 4m/s (Fig. 7, a-b). Due to impingement of the liquid jet on the particle bed, liquid is transferred to the particles (Fig. 7, b), which then propagate the liquid due to particle-particle contacts (Fig. 7, c-d). Some amount of the liquid droplets which does not impinge on the particle bed is carried apart by a (secondary) gas flow in cylinder axis direction (Fig. 7 b-d). The liquid mass carried by the particles is depicted by the blue-white-red colour-bar. While the particles and droplets are depicted in Fig. 7, the fluid phase, as well as the exchange fields are depicted in Fig.8. Due to the momentum coupling with the droplet phase, the motion of the fluid is induced by the droplets and particles respectively (Fig. 8, lower right). The amount of volume occupied by the particles, described by the void fraction is shown on the lower left side of Fig.8. The droplet-particle liquid transfer rate, which has its maximum at the droplet impingement regions is shown on the upper left of Fig.8.

The material properties for the test case are given in Tab. 2.

Parameters	Value
Particle shape	spherical
Particle diameter d_p [m]	0.005
Particle density ρ_p [kg/m^3]	200
Rolling friction coefficient [-]	0.1
Density of water ρ_w [kg/m^3]	998.2
Viscosity of water μ_w [$\text{kg}/(\text{m s})$]	1×10^{-3}
Density of air ρ_a [kg/m^3]	1.2047
Viscosity of air μ_a [$\text{kg}/(\text{m s})$]	1.78×10^{-5}
Surface tension σ_w [N/m]	0.0727

Table 2: Particle and fluid properties.

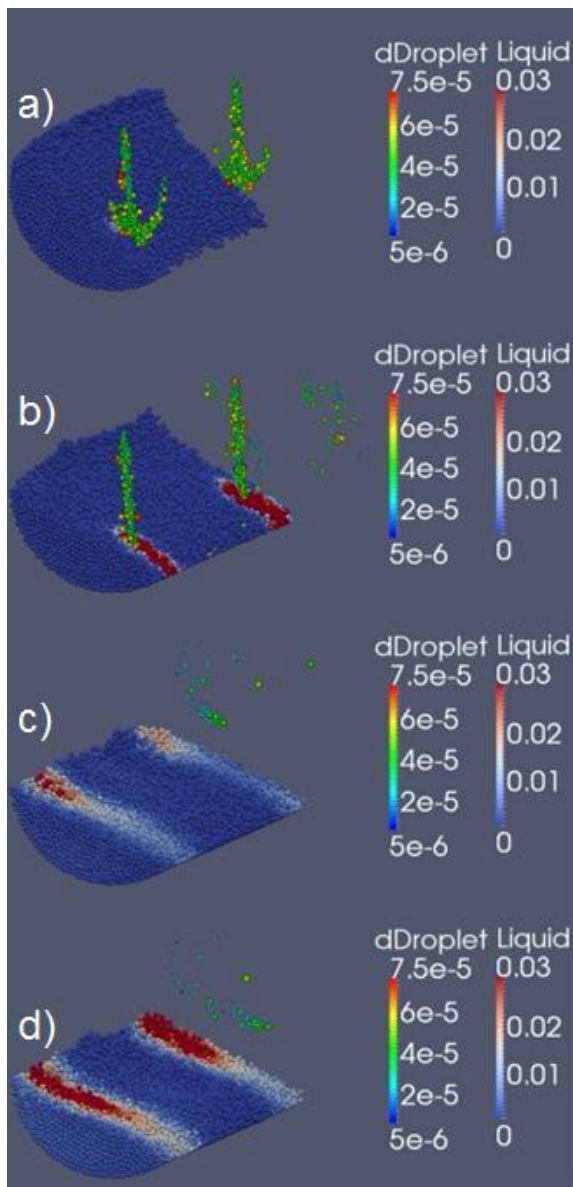


Figure 7: Liquid transfer from droplets to particles as well as particle-particle liquid transfer for a) $t=0.35s$, b) $t=3.5s$, c) $t=5.75s$, e) $t=11s$.

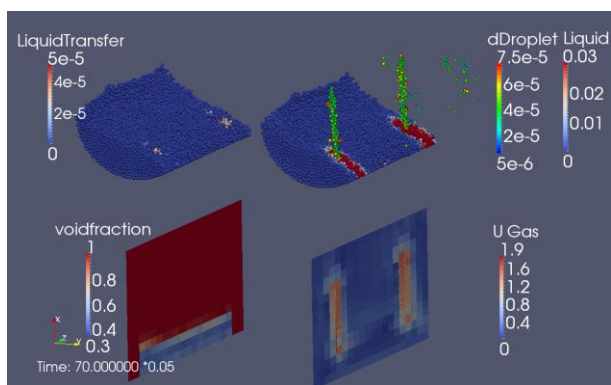


Figure 8: Droplet-particle liquid transfer rate (upper left), droplets and liquid carried on particle surface (upper right), voidfraction field (lower left) and gas velocity (lower right).

CONCLUSION

Within this study a model approach for three phase flow including droplets, particles and a fluid phase was presented. Therefore a coupled CFD-DEM approach was extended by a Lagrangian parcel approach to track parcels of droplets. Dedicated sub-models for droplet-particle liquid transfer as well as a wet particle contact models were presented. The feasibility of this model approach could be shown by applying it to a rotating pan coater. A main advantage of this model approach, is its realisation at a meso-scale level. Spray and particle handling is resolved at a very detailed level capturing many physical effects. This allows for applying this model to many different applications in metallurgical or process industries. After this first stage of model development, sound validation work accompanied by experimental tests, suited to the application, should be conducted. All simulations were realised within an open source framework (CFDEMcoupling, 2011) and ran fully parallel. This allows for simulations at bigger, industrial scales.

ACKNOWLEDGEMENTS

The authors would like to thank the community of CFDEMcoupling (2011) for giving important input and contributions to the development of this open source project. Further we want to thank the C.D. Research Association, the Federal Ministry of Economy, Family and Youth and the National Foundation for Research, Technology and Development.

REFERENCES

- AI, J., CHEN, J.F., ROTTER, J.M., & OOI, J.Y., (2011), "Assessment of rolling resistance models in discrete element simulations", *Powder Technology*, **206**(3), 269-282.
- AMSDEN, A.A., (1985), "KIVA-II: a computer program for chemically reactive flows with sprays", *Los Alamos National Laboratory Report*, LA-11560-MS
- CFDEMcoupling (2011). *CFDEM — Open source CFD, DEM and CFD*. Retrieved October 20, 2011, from <http://www.cfdem.com>
- CROWE, C.T., (1977), "The particle-source-in cell (PSI-CELL) model for gas-droplet flows", *Journal of Fluids Engineering*, **99**, No. 3, pp. 325–332.
- CUNDALL, P.A., & STRACK, O.D. (1979). "A discrete numerical model for granular assemblies." *Geotechnique*, **29**, 47-65.
- DARABI, P., POUATCH, K., SALCUDEAN, M. and GRECOV D., (2008), "DEM investigations of fluidized beds in the presence of liquid coating", *Powder Technology*, **214**, 365-374.
- DEEN, N.G., van SINT ANNALAND, M., van der HOEF, M.A., & KUIPERS, J.A.M., (2007). "Review of discrete particle modeling of fluidized beds", *Chemical Engineering Science*, **62**(1-2), 28-44.
- Di RENZO, A., & Di MAIO, F.P., (2004), "Comparison of contact-force models for the simulation of collisions in DEM-based granular flow codes", *Chemical Engineering Science*, **59**, 525-541.
- DUBEY, A., HSIA, R., SARANTEAS, K., BRONE D., MISRA, T. and MUZZIO, F.J., (2011), "Effect of speed, loading and spray pattern on coating variability in a pan coater", *Chemical Engineering Science*, **66**, 5107-5115.

FRIES, L., ANTONYUK, S., HEINRICH S. and PALZER S., (2011), „DEM-CFD modeling of a fluidized bed spray granulator“, *Chemical Engineering Science*, **66**, 2340-2355

GOLDSCHMIDT, M.J.V., WEIJERS, G.C.C., BOEREFIJN, R., KUIPERS, J.A.M., (2003), “Discrete element modelling of fluidised bed spray granulation”, *Powder Technology*, **138**, 39-45.

GONIVA, C., KLOSS, C. and PIRKER, S., (2009), “Towards fast parallel CFD-DEM: An open-source perspective”, In *Proceedings of Open Source CFD International Conference*, Barcelona, Spain.

GONIVA, C., TUKOVIC, Ž., FEILMAYR, C. and PIRKER, S., (2010), ‘Towards efficient simulation of off-gas scrubbing by a hybrid Eulerian–Lagrangian model’, *Progress in Computational Fluid Dynamics*, **10**, 265-274

GONIVA, C., KLOSS, C., DEEN, N.G., KUIPERS, J.A.M., and PIRKER, S., (2012), “Influence of rolling friction on single spout fluidized bed simulation”, *Particology*, DOI 10.1016/j.partic.2012.05.002.

JASAK, H., (1996), “Error analysis and estimation for the finite volume method with applications to fluid flows.” Doctoral dissertation, Imperial College, London.

KLOSS, C., GONIVA, C., HAGER, A., AMBERGER, S. and PIRKER, S., (2012) “Models, Algorithms and Validation for OpenSource DEM and CFD-DEM”, *Progress in Computational Fluid Dynamics*, **12**, No.2/3 , pp.140 – 152.

KOCH, D.L., and HILL, R.J., (2001), “Inertial effects in suspension and porous-media flows”, *Annual Review of Fluid Mechanics*, **33**, 619-647.

LAMMPS (2009). “LAMMPS user manual. Sandia National Laboratories”, USA. Retrieved October 20, 2011, from <http://lammmps.sandia.gov/doc/Manual.html>

LIGGGHTS (2011). “LAMMPS improved for general granular and granular heat transfer simulations.” Retrieved October 20, 2011, from <http://www.liggghts.com>

OpenCFD Ltd. (2009), “OpenFOAM — The open source CFD toolbox.” Retrieved October 20, 2011, from <http://www.openfoam.com>

O’ROURKE, P.J., (1987), ‘The TAB method for numerical calculations of spray droplet breakup’, Tech. Rep. 872089, *SAE Technical Paper*.

PLIMPTON, S.J., (1995), “Fast parallel algorithms for short-range molecular dynamics”, *Journal of Computational Physics*, **117**, 1-19. (LAMMPS homepage: <http://lammmps.sandia.gov>).

POESCHEL, T., and SCHWAGER, T., (2005), *Computational granular dynamics*. New York: Springer.

SAHNI, E. and CHAUDHURI, B., (2011), “Experiments and numerical modelling to estimate the coating variability in a pan coater”, *International Journal of Pharmaceutics*, **418**, 286-296.

SHI, D. and MCCARTHY, J.J. (2008), “Numerical simulation of liquid transfer between particles”, *Powder Technology*, **184** (1), 64–75.

TSUIJ, Y., KAWAGUCHI, T., & TANAKA, T., (1993), “Discrete particle simulation of two-dimensional fluidized bed”, *Powder Technology*, **77**, 79-87.

van BUIJTENEN, M.S., DEEN, N. G., HEINRICH, S. ANTONYUK, S. and KUIPERS, J.A.M., (2008), “A discrete element study of moisture dependent particle-particle interaction during granulation in a spout fluidized bed”, *6th International Conference on CFD in Oil & Gas, Metallurgical and Process Industries*, SINTEF/NTNU, Trondheim, Norway.

ZHU, H.P., ZHOU, Z.Y., YANG, R.Y., & YU, A.B. (2007). “Discrete particle simulation of particulate systems: Theoretical developments.” *Chemical Engineering Science*, **62**, 3378-3396.

ZHU, H.P., ZHOU, Z.Y., YANG, R.Y., & YU, A.B., (2008), “Discrete particle simulation of particulate systems: A review of major applications and findings”, *Chemical Engineering Science*, **63**, 5728-5770.

ZHOU, Z. Y.; KUANG, S. B.; CHU, K. W.; YU, A. B., (2010), “Discrete particle simulation of particle-fluid flow: model formulations and their applicability”, *Journal of Fluid Mechanics*, **661**, pp. 482-51